ORIGINAL PAPER

Epoxidation of Tall Oil Fatty Acids and Tall Oil Fatty Acids Methyl Esters Using the SpinChem® Rotating Bed Reactor
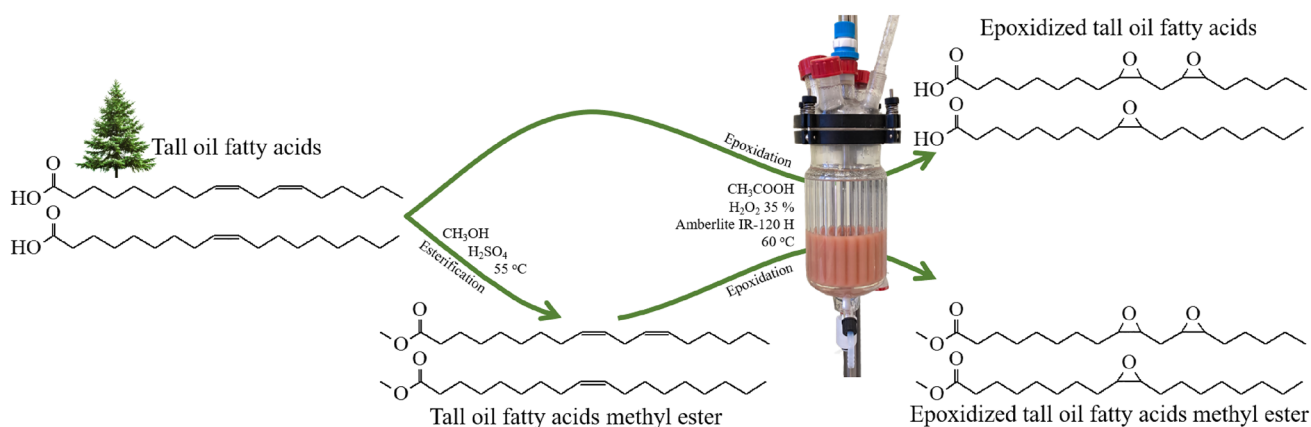
Krzysztof Polaczek[1] · Eliza Kaulina[2] · Ralfs Pomilovskis[2,3] · Anda Fridrihsone[2] · Mikelis Kirpluks[2]

Abstract

Tall oil fatty acids are a second-generation bio-based feedstock finding application in the synthesis of polyurethane materials. The study reported tall oil fatty acids and their methyl esters epoxidation in a rotating packed bed reactor. The chemical structure of the synthesized epoxidized tall oil fatty acids and epoxidized tall oil fatty acids methyl ester were studied by Fourier-transform infrared spectroscopy. Average molecular weight and dispersity were determined from gel permeation chromatography data. The feasibility of multiple uses of the Amberlite® IRC120 H ion exchange resin as a catalyst was investigated. Gel permeation chromatography chromatograms of epoxidized tall oil fatty acids clearly demonstrated the formation of oligomers during the epoxidation reaction. The results showed that methylation of tall oil fatty acids allows obtaining an epoxidized product with higher relative conversion to oxirane and much smaller viscosity than neat tall oil fatty acids. Epoxidation in a rotating packed bed reactor simplified the process of separating the catalyst from the reaction mixture. The Amberlite® IRC120 H catalyst exhibited good stability in the tall oil fatty acids epoxidation reaction.

Graphical Abstract

✉ Krzysztof Polaczek
krzysztof.polaczek@doktorant.pk.edu.pl

1 Department of Chemistry and Technology of Polymers, Cracow University of Technology, Warszawska 24, 31-155, Cracow, Poland

2 Polymer Laboratory, Latvian State Institute of Wood Chemistry, Dzerbenes st. 27, Riga 1006, Latvia

3 Institute of Technology of Organic Chemistry, Faculty of Materials Science and Applied Chemistry, Riga Technical University, P. Valdena St. 3/7, Riga 1048, Latvia

Introduction

The synthesis of polymeric materials with the principles of sustainability and cleaner production has been a widely researched topic in recent years. These principles are intended to reduce the environmental impact of products and production by reducing the use of fossil-based raw materials and replacing them with bio-based or waste/recycled

resources; reducing energy consumption through the use of more efficient processes and equipment; reducing or eliminating toxic and harmful raw materials; reducing the amount and toxicity of waste [1].

A widely available bio-based raw material with high potential in chemical synthesis is crude tall oil (CTO). CTO is a by-product of the wood pulp industry generated at an average rate of 30–50 kg per 1000 kg of processed wood [2]. World production of CTO is between 1.6 and 2 million tonnes/year, of which approximately 650 000 tonnes/year is produced in Europe [3]. CTO contains 30–50 wt.% of free fatty acids (mainly oleic and linolic acid), 15–35 wt.% of rosin acids and residues composed of sterols, fatty alcohols, phenols and hydrocarbons. CTO can be burned as an alternative to heavy fuel oil. However, CTO also can be used as a high-value feedstock for chemical syntheses after separation into various fractions, i.e. tall oil fatty acids (TOFA) and tall oil rosins (TOR). TOR are used as an ingredient in printing inks, adhesives, soaps, detergents, emulsifiers, sealing waxes and soldering fluxes [4]. TOFA is mainly used as a feedstock to produce tall oil fatty acids methyl ester (TOFAME) used as an alternative to diesel fuel [5]. TOFA can also be converted to hydrocarbons by hydrodeoxygenation/decarboxylation reactions [6, 7].

Moreover, TOFA also has been investigated as a potential raw material for the synthesis of bio-based polyols (bio-polyols). Polyols, conventionally petrochemical based, are one of the main components for the production of polyurethanes [8, 9]. The global market for polyols in 2019 was US$26.2 billion, and further growth is expected [10]. Commercially produced polyols are mainly made from non-renewable petrochemical feedstocks. In recent years, there has been an increase in the availability of commercial bio-polyols made from vegetable oils such as castor oil, soybean oil and palm oil [10, 11].

TOFA has several advantages in comparison to vegetable oil-based polyols. A significant advantage of TOFA is the high iodine value (about 155 g I_2/100 g) compared to vegetable oils (e.g., the iodine value of palm oil is 44–58 g I_2/100 g; the iodine value of rapeseed oil is 94–120 g I_2/100 g; the iodine value of soybean oil is 117–143 g I_2/100 g [12]). The higher iodine value indicates more unsaturated double bonds in the structure of fatty acids that can be chemically modified [13]. Moreover, TOFA is a second-generation feedstock and do not pose a concern about competition with food and feed supplies.

The most commonly used method for synthesizing bio-polyols from TOFA is a two-step process of epoxidation followed by oxirane ring-opening with proton donors [14]. The classical Prilezhaev epoxidation method uses peroxycarboxylic acids formed *in-situ* to oxidize the double bonds. Formic acid or acetic acid and hydrogen peroxide are most commonly used in this process [15]. The main disadvantage of the epoxidation of fatty acids is that the carboxyl groups of fatty acids react with hydrogen peroxide to form peroxy fatty acids which act as oxygen carriers, leading to extensive oxirane ring-opening and formation of oligomeric products [16, 17]. The use of heterogeneous catalysts such as acid ion exchange resins helps to reduce the occurrence of oxirane ring-opening side reactions compared to the use of heterogeneous catalysts such as H_2SO_4 [18, 19]. Heterogeneous catalysts can be easily separated from the reaction mixture, washed and reused, thus reducing process costs [20, 21].

A modern type of reactor that can facilitate the process of separating the catalyst from the reaction mixture is the rotating packed bed reactor (RBR), in which the catalyst is separated from the rest of the reaction mixture. The mixing occurs due to the centrifugal force generated by a rotating catalyst container. The use of the RBR leads to reduced energy consumption and the water needed to separate the catalyst from the reaction mixture. The literature describes studies where RBR was used for epoxidation of vegetable oils using ion exchange resin under conventional heating [22], oleic acid, TOFA and distilled tall oil under microwave irradiation [23], as well as epoxidation of oleic acid in the presence of ultrasound irradiation [24].

Polymer laboratory at Latvian State Institute of Wood Chemistry has studied the epoxidation of TOFA before. Kirpluks et al. studied the epoxidation process of TOFA under conventional heating [9, 17]. Studies on the epoxidation of TOFA using in-situ formed peracetic acid, catalyzed by the Amberlite® IRC120 H ion exchange resin, have confirmed that the resulting epoxidized TOFA is a mixture of monomers, dimers, trimers and oligomers [14, 17, 19]. Thus, the bio-polyols synthesized from ETOFA exhibited high viscosity, which significantly limits their potential application. The high viscosity of bio-polyols is undesirable as it complicates the large-scale production of rigid polyurethane foams [14].

The objective of this article was to compare the epoxidation of neat TOFA and their methyl ester with the use of an RBR reactor. Esterification of TOFA could help to reduce the occurrence of undesirable side reactions. The epoxidation reactions were carried out using varying catalyst content of 10, 15, 20 and 25 wt.%. The stability and reusability of the catalyst were also tested. The following characteristics were determined for obtained products: epoxy value, acid value and viscosity. The chemical structure of epoxidized TOFA and epoxidized TOFAME were studied by Fourier transform infrared spectroscopy and gel permeation chromatography.

Materials and Methods

Materials

The following reagents were used for synthesizing epoxidized TOFA and epoxidized TOFAME: TOFA (trade name

"FOR2") with a high content of fatty acids (> 96%), low content of rosin acids (1.9%), and unsaponifiables (1.8%) was ordered from Forchem Oyj (Rauma, Finland). The initial acid and iodine values for TOFA were 198 ± 1 mg KOH/g and 155 ± 1 g I_2/100 g, respectively. Acetic acid (AcOH), puriss. p.a., ACS reagent, reag. ISO, reag. Ph. Eur., $\geq 99.8\%$ was ordered from Fluka (Seelze, Germany). Ethyl acetate (EtOAc), puriss., meets the analytical specifications of Ph. Eur., BP, NF, $\geq 99.5\%$ (GC) was ordered from Riedel–de Haen (Seelze, Germany). Amberlite® IRC120 H, strongly acidic, hydrogen form, hydrogen peroxide (H_2O_2) 35%, methanol (MeOH), puriss. p.a., ACS reagent, reag. ISO, reag. Ph. Eur., $\geq 99.8\%$ from Riedel–de Haen (Seelze, Germany), and sulfuric acid (H_2SO_4), puriss., meets the analytical specifications of Ph. Eur., BP, 95–97% were ordered from Sigma-Aldrich (Steinheim, Germany).

The following reagents were used for the analysis of TOFA and synthesized products: potassium hydroxide (KOH), ACS reagent, $\geq 85\%$, pellets, potassium phthalate monobasic (KHP), ACS reagent, acidimetric standard, chloroform, puriss. p.a., reag. ISO, reag. Ph. Eur., 99.0–99.4% (GC), perchloric acid, puriss. p.a., ACS reagent, reag. ISO, reag. Ph. Eur., 70.0–72.0%, tetraethylammonium bromide, reagent grade, 98%, acetic anhydride, puriss. p.a., ACS reagent, reag. ISO, reag. Ph. Eur., $\geq 99\%$ (GC), N,N-dimethylformamide (DMF), anhydrous, 99.8%, 4-(dimethylamino) pyridine (DMAP), ReagentPlus, $\geq 99\%$, and potassium iodide (KI), ACS reagent, $\geq 99.0\%$ were obtained from Sigma-Aldrich (Steinheim, Germany). Methanol (MeOH), puriss. p.a., ACS reagent, reag. ISO, reag. Ph. Eur., $\geq 99.8\%$, and dichloromethane, puriss. p.a., ACS reagent, reag. ISO, $\geq 99.9\%$ were ordered from Riedel–de Haen (Seelze, Germany). Hanus solution, volumetric 0.1 M IBr, acetic acid (AcOH), puriss. p.a., ACS Reagent, Reag. ISO, Reag. Ph. Eur., $\geq 99.8\%$, and crystal violet, an indicator for determining the redox potential, S. No.:785 were ordered from Fluka (Seelze, Germany). Cresol red, indicator grade, was obtained from Alfa Aesar (Kandel, Germany). Sodium thiosulfate 0.1 mol/l (0.1 N) was ordered from Chempur (Karlsruhe, Germany).

Synthesis of TOFAME

The methylation of TOFA was carried out in a 2 l three-necked round bottom flask. The flask was immersed in a water bath equipped with a stirrer, a thermocouple, and a reflux condenser. The reaction conditions were chosen based on literature data [25]. The reaction temperature was 55 °C, and the reaction time was 30 min. The molar ratio of methanol to TOFA double bonds was 6:1. Catalyst content was 0.5 wt.% of TOFA. At first, 900 g of TOFA was added to the flask. The flask was immersed in the water bath, and the catalyst-methanol mixture (4.5 g of H_2SO_4 and 600 g

MeOH) was added to the TOFA and stirred (100 rpm) under reflux. The reaction start time was assumed when the mixture reached the set temperature of 55 °C. After the reaction was completed, the mixture was poured into a separating funnel, and about 100 ml EtOAc was added. The bottom water-waste phase was poured out. The upper organic phase consisting of TOFAME was washed four times with warm distilled water at a temperature of 55 °C and then dried using a rotatory vacuum evaporator.

Synthesis of Epoxidized TOFA and Epoxidized TOFAME

Epoxidation was carried out using TOFA and TOFAME, resulting in epoxidized tall oil fatty acids (ETOFA) and epoxidized tall oil fatty acids methyl ester (ETOFAME). The synthesis scheme is given in Fig. 1.

The epoxidation of TOFA was carried out in a 1200 ml RBR, model V3 manufactured by Spinchem® (Sweden), as shown in Fig. 1. The reaction vessel is made of borosilicate glass. The rotating bed with a diameter of 70 mm and a height of 30 mm, the catalyst separation filter with a porosity of 104 μm and the shaft are made of stainless steel. The RBR was equipped with a heating/cooling jacket and a bottom drain. A thermocouple, dropping funnel, and a reflux condenser were attached to the 5-neck lid. A rotating bed filled with ion exchange resin was also used as a stirrer. The epoxidation of TOFA was carried out using peroxyacetic acid generated *in-situ* in the reaction of AcOH and H_2O_2 and using ion exchange resin as a catalyst. The molar ratio of TOFA double bonds to H_2O_2 to AcOH was 1.0:1.5:0.5. The mass of the catalyst was kept constant (40 g), while variable catalyst content of 10, 15, 20, and 25 wt.% in relation to the TOFA content was used.

At first, the calculated amount of TOFA and AcOH was added to the reactor. The initial set temperature of the jacket was 40 °C. The speed of the RBR was set to 400 rpm, and the mixture was started to stir. The calculated mass of H_2O_2 was added to the dropping funnel. After the reaction mixture reached a temperature of 40 °C, H_2O_2 was added during 60 min. The reaction temperature was increased by 5 °C at intervals of 15 min, finally setting the reaction temperature to 60 °C and running the reaction for 7 h total. The temperature of the reaction mixture did not exceed the set temperature by more than 2 °C. During the epoxidation, small amounts of product were collected every h by the bottom drain of RBR for analysis. Products were washed by adding EtOAc and warm distilled water at a temperature of 55 °C. The organic phase was washed 3 times with the addition of distilled water in a separating funnel. Products were dried using a rotatory vacuum evaporator to remove water and EtOAc residues. Fresh ion exchange resin was used for every

Fig. 1 The synthesis scheme of epoxidized TOFA or TOFAME
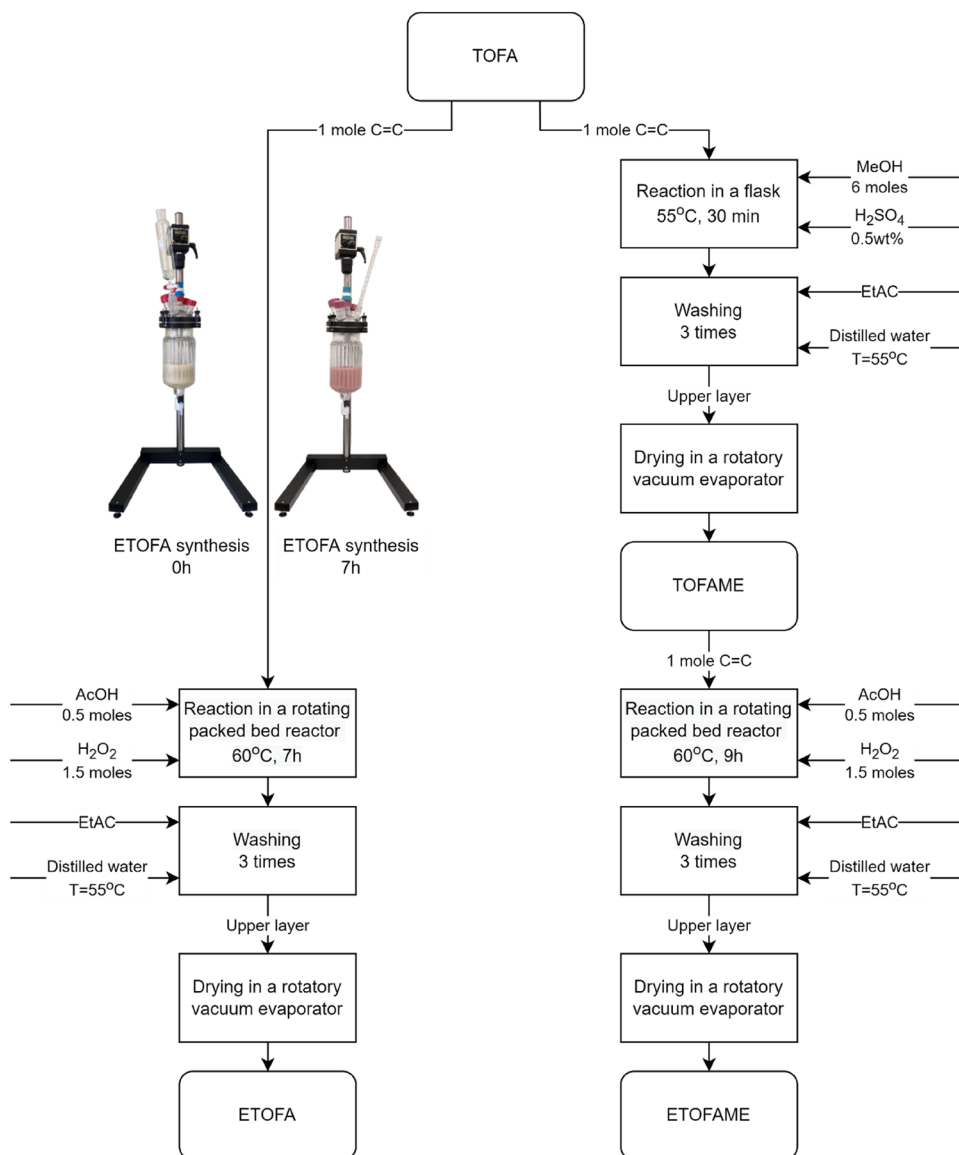
reaction. Reagent weights for TOFA or TOFAME epoxidation are given in Table 1.

The epoxidation synthesis of TOFAME was carried out in the same way as the TOFA epoxidation reaction. The overall reaction time was extended to 9 h to obtain additional information about the synthesis.

Reusability of Amberlite® IRC120 H Ion Exchange Resin in the Epoxidation of TOFA

Ten epoxidation reactions were performed to determine the reusability of the catalyst. Syntheses of ETOFA were carried out as described in Sect. "Synthesis of Epoxidized TOFA and Epoxidized TOFAME" with the difference that the catalyst was not removed from the synthesis media. The catalyst load for TOFA epoxidation was 20 wt.%. The reaction time

Table 1 Reagent weights for TOFA or TOFAME epoxidation

Catalyst content*, wt.%	TOFA or TOFAME, g	H_2O_2, g	AcOH, g
10	400.0	356.1	74.1
15	266.7	237.4	49.4
20	200.0	178.1	37.0
25	160.0	142.4	29.6

*Catalyst content as weight percent from TOFA or TOFAME

was reduced to 4 h. The design of the RBR reactor allows the catalyst to be separated from the reaction mixture without any losses and additional operations such as filtration, washing and drying, as is the case when a batch reactor is used [19]. Separation of the reaction mixture from the catalyst in

the RBR reactor involves solely pouring it out through the bottom drain.

Methods of Analysis

The iodine value (IV) was determined according to ISO 3961:2018, and it is calculated by using Eq. (1).

$$IV = \frac{(V_b - V_s) \cdot c_t \cdot 12.69}{m_s} gI_2/100g \qquad (1)$$

where V_b and V_s are volumes of sodium thiosulfate required for the blank and the sample, in ml, c_t is the concentration of sodium thiosulfate, in mol/l, m_s is the mass of the sample, in g. 12.96 is the conversion factor from milliequivalents sodium thiosulfate to grams of iodine.

Iodine value was used to determine fatty acid unsaturation (n_{db}, moles of double bonds in gram of oil) by using Eq. (2).

$$n_{db} = \frac{IV}{M_{I_2} \cdot 100} mol/g \qquad (2)$$

where M_{I2} is the molar mass of I_2, in g/mol.

The epoxy value (EV) (the content of oxirane rings) was determined according to ASTM D1652-11(2019) standard. Epoxy group content in moles per 100 g of oil was calculated by using Eq. (3).

$$EV = \frac{V_t \cdot c_t}{m_s \cdot 10} mol/100g \qquad (3)$$

where V_t is volume, in ml, of titrant used, c_t is titrant concentration, in mol/l, m_s is mass of the sample.

The percentage of relative conversion of unsaturated bonds to oxirane (RCO) was calculated by Eq. (4) [26].

$$RCO = \frac{OO_{ex}}{OO_{th}} \cdot 100\% \qquad (4)$$

where OO_{ex} is the experimentally determined content of oxirane (%), calculated by Eq. (5). The OO_{th} is the theoretical maximum oxirane content of oxirane in 100 g of fatty acids (%), which was calculated by Eq. (6).

$$OO_{ex} = A_O \cdot EV\% \qquad (5)$$

where A_o is the atomic mass of oxygen.

$$OO_{th} = \frac{\left(\frac{IV_0}{2A_i}\right) \cdot A_o}{100 + \left(\frac{IV_0}{2A_i}\right) \cdot A_o} \cdot 100 \qquad (6)$$

where A_i is the atomic mass of iodine, and IV_o is the initial iodine value of the fatty acid sample.

The relative ethylenic unsaturation (REU) was calculated by Eq. (7):

$$REU = \left(\frac{IV_{ex}}{IV_o}\right) \cdot 100\% \qquad (7)$$

where IV_o is the initial iodine value, and IV_{ex} is the remaining iodine value during synthesis.

Hydroxyl value (HV) was determined according to ISO 4629–2:2016 standard and calculated by Eq. (8).

$$HV = \frac{(V_b - V_s) \cdot c_t \cdot 56.106}{m_s} mgKOH/g \qquad (8)$$

where V_b, V_s are volumes, in ml, of potassium hydroxide required for the blank and the sample, respectively, c_t is the concentration of KOH, in mol/l m_s is the mass of the sample, in g. 56.106 is the molar mass of KOH, g/mol.

Acid value (AV) was determined according to ASTM D1980-87(1998) standard and calculated by Eq. (9).

$$AV = \frac{V_t \cdot c_t \cdot 56.106}{m_s} mgKOH/g \qquad (9)$$

where V_t is the volume of titrant used, in ml, c_t is the concentration of KOH, in mol/l, m_s is the mass of the sample, in g. 56.106 is the molar mass of KOH, g/mol.

From the determined relative conversion to oxirane (Eq. 4) and relative ethylenic unsaturation (Eq. 7), the selectivity (S) of TOFA and TOFAME epoxidation reaction was calculated according to Eq. 10.

$$S = \frac{RCO}{100\% - REU} \qquad (10)$$

The viscosity was measured at 25 °C using the Thermo Science HAAKE (Medium–High Range Rotational Viscometer, Thermo Fisher Scientific, Waltham, MA, USA).

The spectroscopic analysis of the chemical structure of the precursors and products was carried out using a Fourier-transform infrared spectrometer (FTIR) model iS50 (Thermo Fisher Scientific, Waltham, MA, USA) at a resolution of 4 cm^{-1} (32 scans) in the infrared range of 4000–500 cm^{-1}. The FTIR data were collected using an attenuated total reflectance (ATR) accessory with a diamond crystal.

An Agilent Infinity 1260 HPLC system (Agilent Technologies, Inc., Santa Clara, CA, USA) with degasser, autosampler, refractive index (RI) detector, and MALS (miniDAWN) detector was used to perform gel permeation chromatography (GPC) analysis. The analysis was performed using two GPC analytical columns connected in series: PLgel Mixed-E (3 uL, 300 × 7.5 mm). The flow rate was 1 ml/min, and the temperature of the RI detector was 35 °C. A total of two duplicate trials were carried out.

Results and Discussion

The epoxidations of TOFA and TOFAME were carried out using peracetic acid generated *in-situ* by the reaction of acetic acid and hydrogen peroxide. The kinetic curves of RCO increase depending on the applied catalyst content are presented in Fig. 2.

In the case of TOFA epoxidation (Fig. 2a), the application of 10 wt.% catalyst content resulted in RCO of 42.5% over a period of 6 h and a decrease in RCO to 40.1% at the seventh hour of the reaction, which corresponds to an EV of 0.237 mol/100 g and 0.223 mol/100 g, respectively. The reduction in the RCO implies that the oxirane ring-opening reactions occurred more intensively than the formation of new epoxy groups after the sixth hour. The increase in the catalyst content led to an increase in RCO to 47.5% after 7 h of the reaction (EV of 0.262 mol/100 g), 49.1% (EV of 0.275 mol/100 g), and 50.4% (EV of 0.281 mol/100 g) for 15, 20 and 25 wt.% of the catalyst content, respectively. The maximum RCO was reached after 5 h of reaction for the 15 and 20 wt.% of the catalyst content, while for the 25 wt.% of the catalyst content after 4 h of reaction. In a comparable experiment conducted in a batch reactor, the maximum RCO value achieved after 5 h of reaction at 20 wt.% catalyst content was 42.9% [19].

The kinetic curves of TOFAME are shown in Fig. 2b. The obtained epoxidized TOFAME exhibited significantly higher RCO in relation to TOFA of 65.2% (EV = 0.337 mol/100 g), 78.6% (EV = 0.406 mol/100 g), 81.0% (EV = 0.419 mol/100 g), 81.2% (EV = 0.420 mol/100 g) for catalyst content of 10, 15, 20 and 25 wt.%, respectively. Methylation of TOFA contributed to reducing side reactions caused by the opening of oxirane rings with a carboxyl group. All kinetic curves except the reaction catalyzed by

10 wt.% catalyst content showed virtually no increase in RCO after 7 h of the epoxidation reaction, which may be caused by side reactions occurring due to the presence of small amounts of fatty acids or by the reactions with acetic acid, peracetic acid, hydrogen peroxide or water [27].

For the TOFAME epoxidation (Fig. 2b), an RCO of about 50% is achieved between 2 and 3 h of reaction at catalyst content > 15 wt.%. In comparison, the same RCO was achieved between 4 and 6 h for TOFA epoxidation at the same catalyst concentrations. The shorter epoxidation time leads to lower costs of the epoxidation process.

The intensity of side reactions is affected by the content of carboxyl groups in the fatty acid. The synthesized TOFAME had an average AV of 39.95 mg KOH/g (the average AV of TOFA was 198.03 mg KOH/g), indicating that not all carboxyl groups were esterified. Figure 3 shows the change in AV during the epoxidation reactions of TOFA (Fig. 3a) and TOFAME (Fig. 3b). The decrease in AV during epoxidation confirmed that carboxyl groups took part in side reactions by opening oxirane rings. The most significant changes in AV were observed for the TOFA epoxidation catalyzed with 25 wt.% catalyst content.

Application of heterogeneous catalysts such as functionalized acidic ion exchange resin in epoxidation reaction provides higher selectivity and reduces side reactions compared to homogeneous catalysts [26]. Small molecules of organic acids can easily diffuse into the structure of porous acidic ion exchange resin, where the formation of peracetic acid occurs. Larger-sized molecules, such as triglycerides, can penetrate the catalyst structure much more restrictedly; thus, the generated oxirane rings are protected from attack by protons confined to the catalyst matrix [28]. The intensive occurrence of side reactions in TOFA epoxidation may suggest that due to their small size, TOFA molecules (about
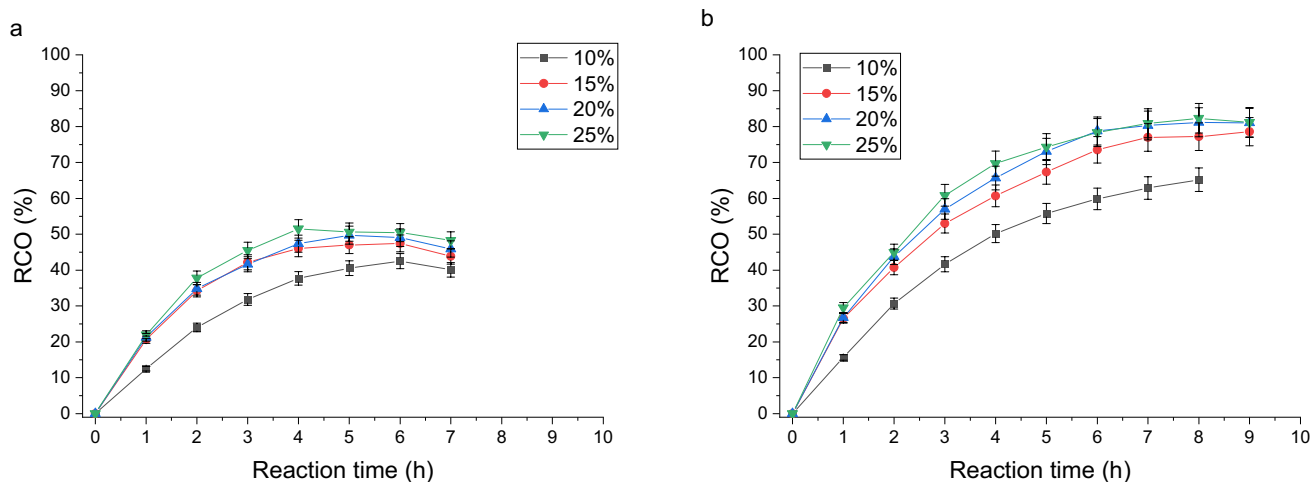

Fig. 2 RCO of TOFA **(a)** and TOFAME **(b)** at different catalyst content (wt.%)
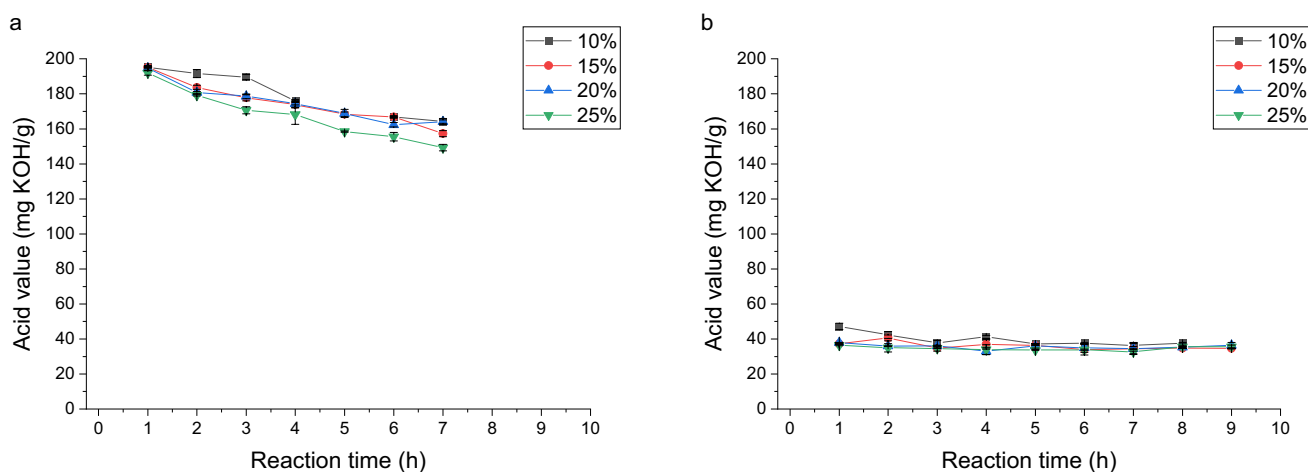
Fig. 3 The change in AV of the TOFA (**a**) and TOFAME (**b**) during the epoxidation process at different catalyst content (wt.%)

3 times smaller than triglyceride) penetrated the catalyst structure.

The TOFA and TOFAME epoxidation reaction may be also influenced by unsaturated fatty acids' composition and chemical structure. Lawer-Yolar et al. reported TOFA composition of 57.7% oleic acid, 35.4% linoleic acid and other mainly saturated fatty acids [25]. Keskin et al. [5] reported TOFA composition of 52.7% oleic acid, 38.3% linolenic acid, 6.9% linolenic acid and 2.1% stearic acid.

A study on the kinetics of the epoxidation of a high-linolenic triglyceride catalyzed by an ion exchange resin showed that the chemical groups (unsaturated and oxirane) at the 9th and 12th positions possess lower reactivity compared to the reactivity of the same groups at the 15th position. Chemical groups at the 15th position are not affected by steric and electronic effects of the glycerol center that highly affected the closer groups (at the 9th and 12th positions). The opening of the epoxy group at the 15th position can cause steric hindrance affecting the epoxidation of the rest of the double bonds but also preventing any interaction between organic acid and the epoxy groups, thus preventing their cleavage [29]. TOFA and TOFAME do not contain glycerol center, which could interact sterically and electrically with chemical groups at the 9th, 12th and 15th positions. However, in the case of TOFA epoxidation reactions, intensive oligomerization reactions leading to an increase in the molecular weight of the molecule can cause a steric hindrance preventing epoxidation of the remaining unsaturated bonds. Such phenomenon, together with the occurrence of side reactions of oxirane ring opening, can be responsible for the low RCO of TOFA epoxidation. The lower AV in the case of TOFAME reduces the formation of dimers and trimer responsible for steric hindrance thus a significantly higher RCO is achieved.

According to La Scala and Wool, rate constants of epoxidation of fatty acids methyl ester increased as the level of

unsaturation increased, therefore oleic acid should undergo relatively slower epoxidation compared to linoleic and linolenic acids. An explanation for this phenomenon is that as the number of unsaturated bonds increases, the electron density increases, resulting in an increase in the reaction rate constant [30].

The change in REU over time at different catalyst content is presented in Fig. 4. The REU of TOFA (Fig. 4a) ranged from 10 to 27% and decreased with increasing catalyst content after 7 h of reaction. The lower the REU value, the more double bonds have reacted. At the same time, low RCO of TOFA (Fig. 2a) (from 40 to 48% depending on catalyst content) combined with low REU confirmed the effect of a high content of carboxyl groups (high AV) on the intensity of the oxirane ring-opening side reaction. The REU of TOFAME (Fig. 4b) ranged from 20 to 33.5% after 7 h of reaction. It was observed that increasing the catalyst content for TOFAME above 15 wt.% has no significant effect on the REU value.

The chemical structures of TOFA during the epoxidation reaction were investigated using FTIR spectroscopy. The overall FTIR of TOFA spectra are shown in Fig. 5a. The =C–H double bond stretching peak with the maximum at 3009 cm^{-1} (Fig. 5a) disappeared during the reaction, while the stretching peak at 823 cm^{-1} originating from the –C–O–C– epoxy groups appeared (Fig. 5a). The close-up of the C–O–C oxirane ring stretching vibration peak (Fig. 5c) shows the gradual increase of epoxy group content in the TOFA structure. The intensity of the epoxidation reaction decreased with time, which correlates with the RCO data (Fig. 2a). The gradual decrease of the =C–H stretching bond at 3009 cm^{-1} is shown in Fig. 5b. The peak practically disappeared, confirming previous REU results (Fig. 4a). Figure 5d shows the decreasing intensity of the stretching peak of the carboxyl groups –C=O at 1707 cm^{-1} while increasing the
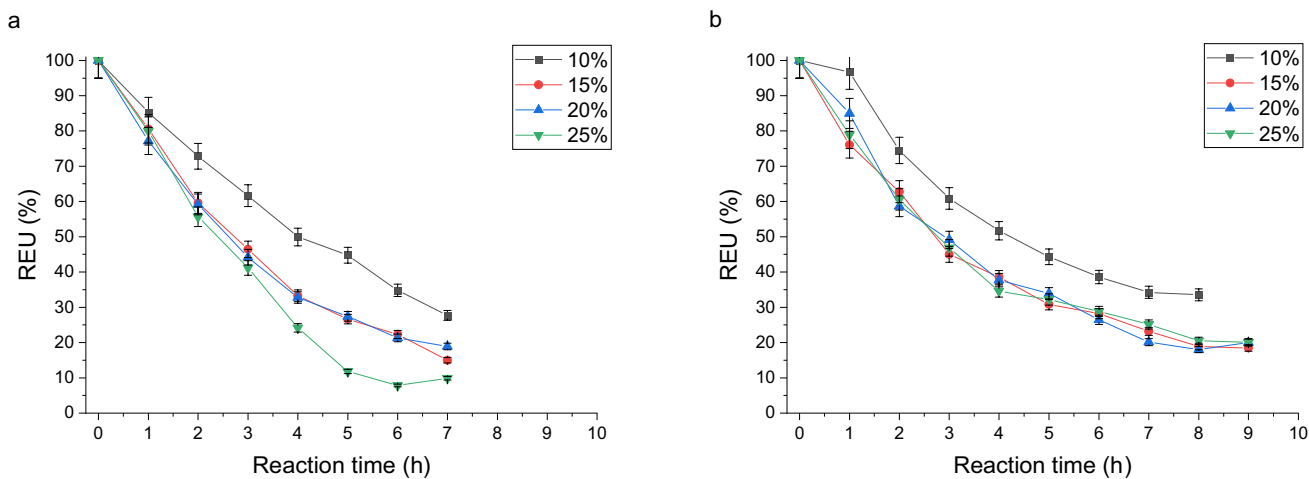
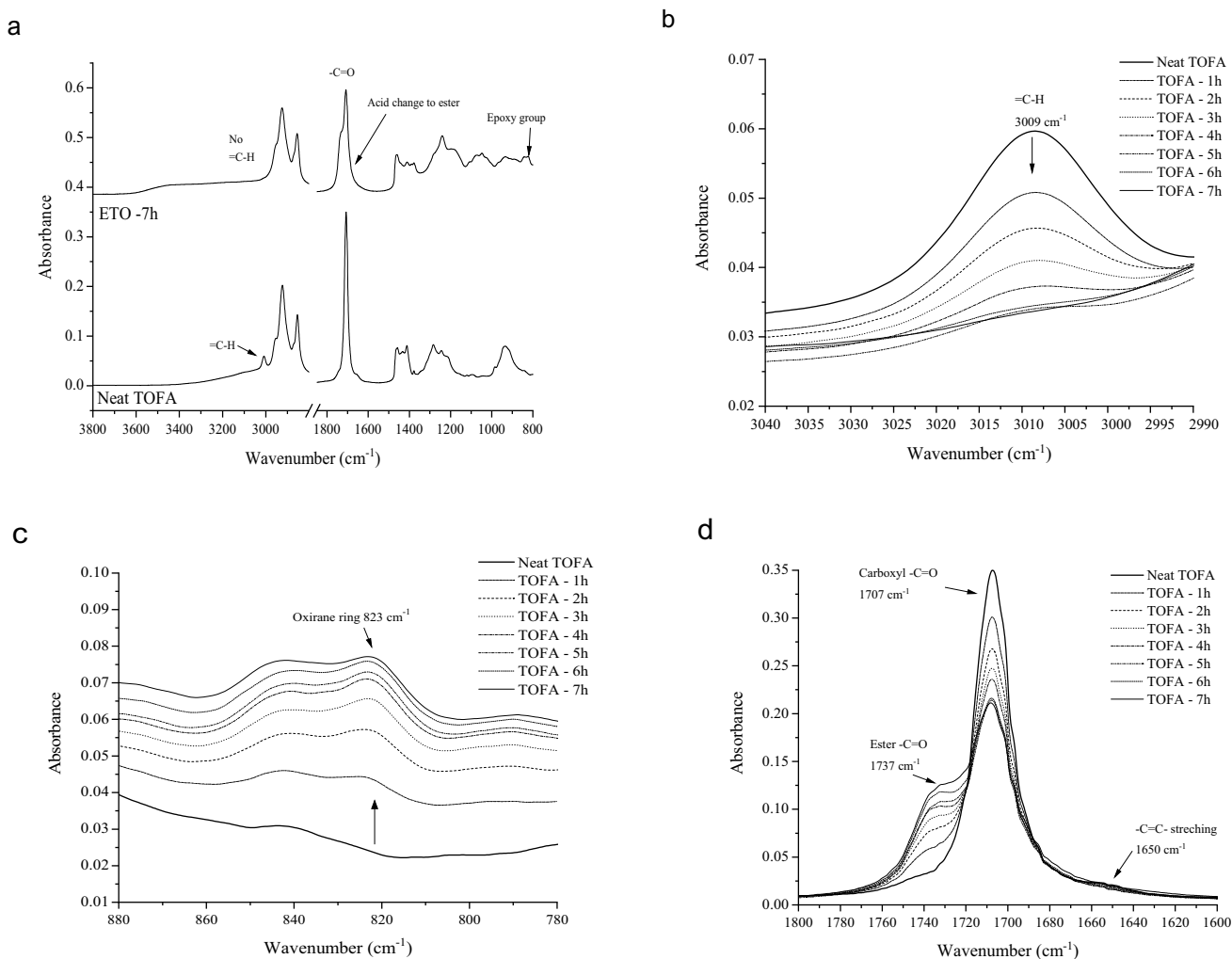**Fig. 4** REU of TOFA (**a**) and TOFAME (**b**) at different catalyst content (wt.%)

Fig. 5 FTIR spectra during TOFA epoxidation over time at 20 wt.% of the catalyst content; **a** overall FTIR spectra; **b** change of double bond absorption band, 3009 cm^{-1}, **c** change of oxirane ring vibration, 823 cm^{-1}, **d** change of carboxyl –C=O stretching vibration absorption band, 1707 cm^{-1}; ester –C=O stretching vibration absorption band, 1737 cm^{-1} and –C=C– stretching vibration band, 1650 cm^{-1}

intensity of the stretching peak vibrations of the ester groups –C=O at 1737 cm^{-1}. This indicates that the carboxyl group of TOFA opens the epoxy group with the formation of an ester group in dimers and molecules with multiples of TOFA molecular weight.

FTIR analysis of TOFAME and its epoxidation products was also performed. The overall FTIR spectra are shown in Fig. 6a. Similar to the TOFA, the =C–H double bond stretching peak at 3009 cm^{-1} (Fig. 6b) disappears almost completely during the reaction while the stretching –C–O–C– epoxy groups peak at 823 cm^{-1} increased (Fig. 6c). Figure 6d shows a close-up of the region of the carboxyl and ester group peak bands. The disappearance of the –C=O carboxyl group peak bands at 1707 cm^{-1} results in the gradual uncovering of the ester group peak band and the shift towards lower wavenumbers.

The initial presence of carboxyl group peak bands confirms their incomplete conversion during the esterification process. Nevertheless, the occurrence of side reactions affecting the increase of molecular weight and viscosity of the products was significantly reduced.

Figure 7a shows the change in TOFA viscosity during the epoxidation with different catalyst content. The initial viscosity of TOFA was 27.26 mPa•s. The resulting epoxidized TOFA synthesized with a catalyst content of 10 wt.% had a viscosity of 956.93 mPa•s. Higher catalyst content led to products with higher viscosities of 2168.00, 1736.10 and 1836.50 mPa•s for synthesis with catalyst content of 15, 20 and 25 wt.%, respectively.

The change in viscosity during TOFAME epoxidation is shown in Fig. 7b. The initial viscosity of TOFAME was 7.36 mPa•s. After 9 h of reaction (2 h longer than TOFA),
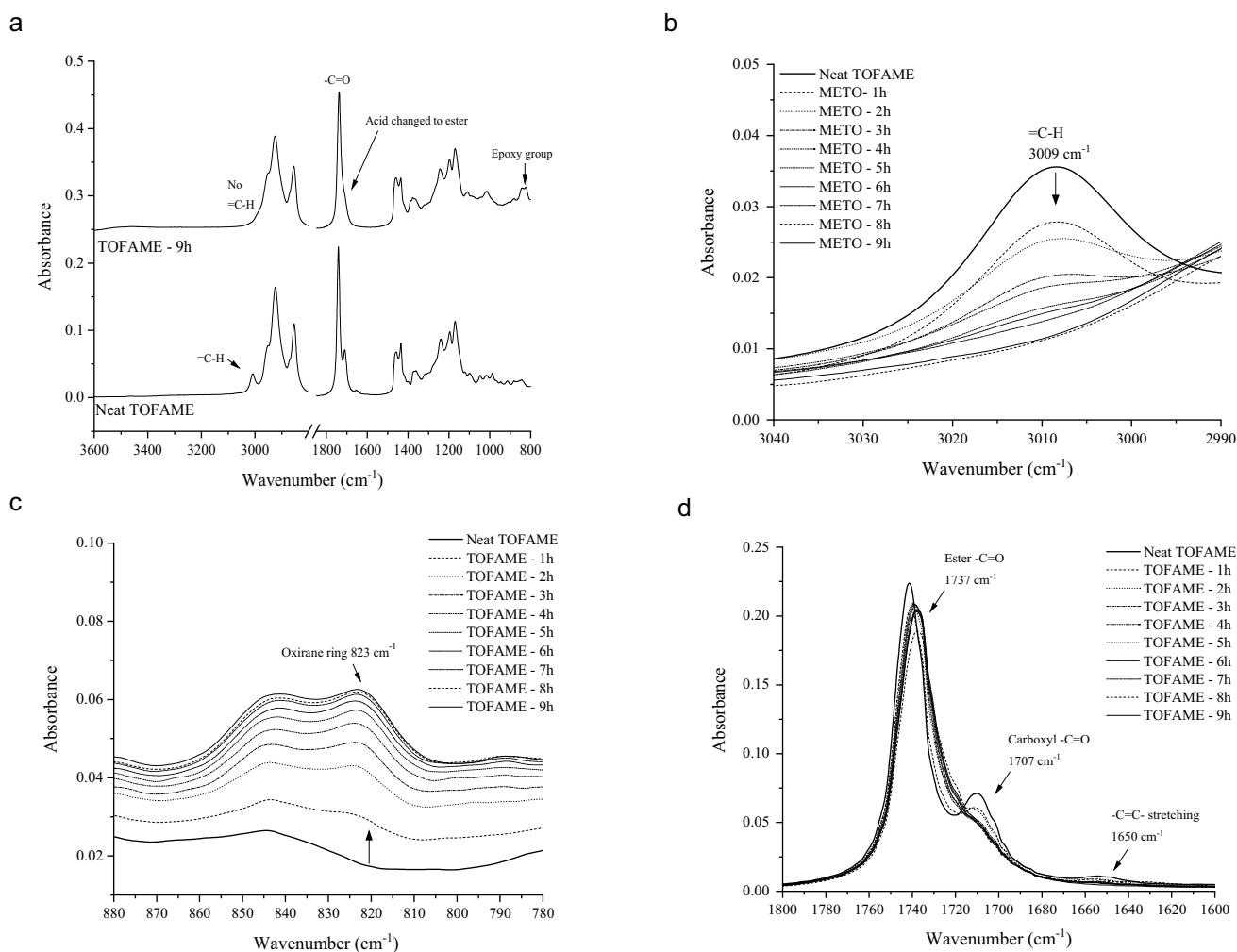

Fig. 6 FTIR spectra during TOFAME epoxidation over time at 20 wt.% of the catalyst content; **a** overall FTIR spectra; **b** change of double bond absorption band, 3009 cm^{-1}, **c** change of oxirane ring vibration, 823 cm^{-1}, **d** change of carboxyl –C=O stretching vibra-tion absorption band, 1707 cm^{-1}; ester –C=O stretching vibration absorption band, 1737 cm^{-1} and –C=C=stretching vibration band, 1650 cm^{-1}
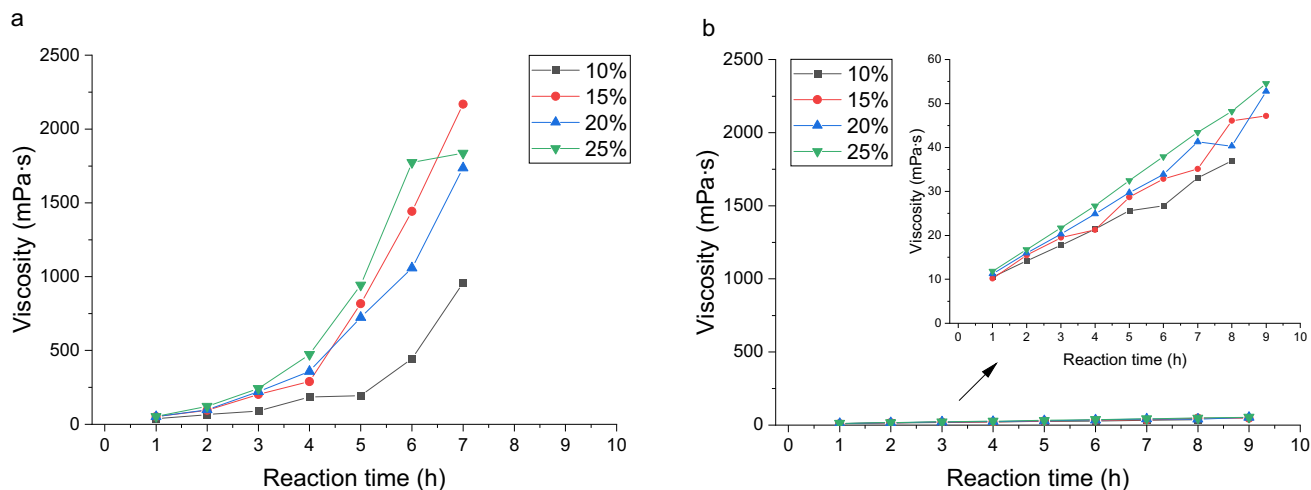
Fig. 7 The viscosity of TOFA **(a)** and TOFAME **(b)** at different catalyst content (wt.%)

the final viscosity ranged from 36.94 mPa•s to 54.55 mPa•s for the reaction catalyzed by 10 wt.% and 25 wt.% catalyst content, respectively. The resulting ETOFAME, despite its high EV, exhibited very low viscosities, being only slightly higher than the initial TOFA viscosity (27.26 mPa•s).

TOFA and TOFAME samples synthesized at 25 wt.% of the catalyst content were analyzed using GPC chromatography. It was necessary to follow the changes in molecular weight to analyze the course of the synthesis and determine the optimal duration of the synthesis. The GPC chromatograms are shown in Fig. 8. During TOFA epoxidation (Fig. 8a), a significant reduction in peak intensity with a retention time of ~15.30 min corresponding to the monomer content is observed. At the same time, the intensity of the peaks characterizing the content of dimers (retention

time ~14.15 min) and trimers (retention time ~13.10 min) increased significantly. This indicates side reactions that occur during epoxidation involving oxirane ring-opening with the carboxyl group of fatty acid. The chromatogram also showed an increase in the peak at retention time ~14.90 min during the process, corresponding to by-products formed during the epoxidation process by oxirane ring-opening with AcOH.

Figure 8b characterizes content during TOFAME epoxidation. The changes in peak intensity are relatively small compared to the TOFA epoxidation process. Although the peak corresponding to the dimers is clearly observed, it is significantly lower in intensity than in the case of TOFA epoxidation, which means that they are formed in much lower content. Significantly fewer by-products, such as
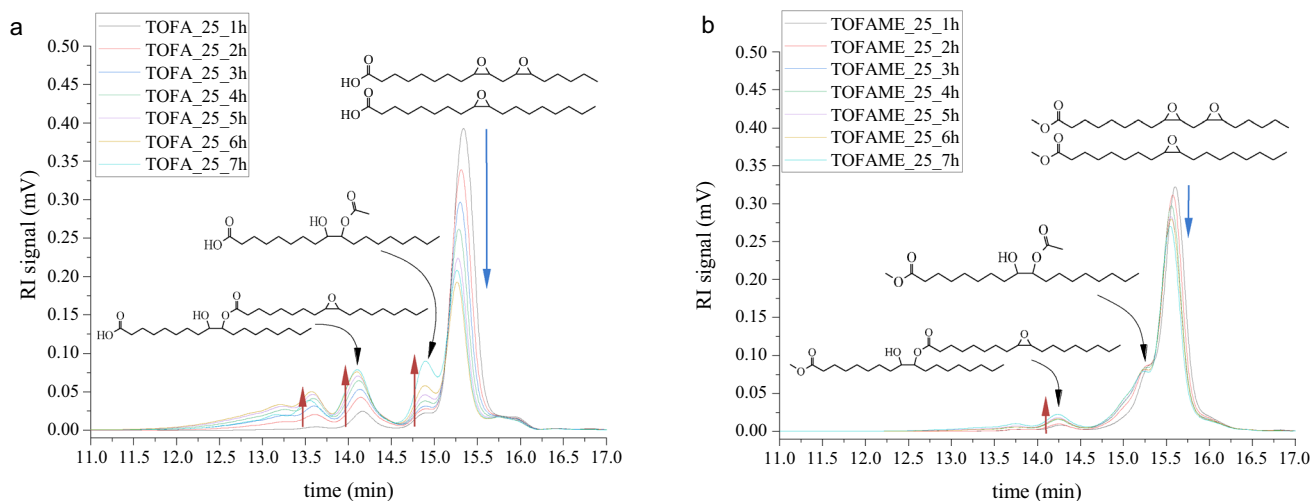

Fig. 8 GPC chromatograms during epoxidation over time at the catalyst content of 25 wt.%; **a** TOFA epoxidation **b** TOFAME epoxidation

dimers and trimers, are formed. The formation of dimers and trimers increases the viscosity of the product and thus makes it difficult to use it in further processing. Therefore, preventing the formation of these undesirable by-products during the synthesis is a significant benefit.

Polydispersity characterizes the molecular weight distribution. The change of polydispersity is shown in Fig. 9. In the case of TOFA epoxidation, the polydispersity increased significantly during the first h of epoxidation, reaching 1.8 in the 4th h. In contrast, the change in dispersity during the oxidation of TOFAME was less pronounced. It indicated greater homogeneity of TOFAME epoxidation products and smaller width of the molecular weight distribution.

Table 2 summarizes the physico-chemical properties of epoxidized TOFA and TOFAME at optimal synthesis time, which is considered to be the time when the reaction reached the highest RCO.

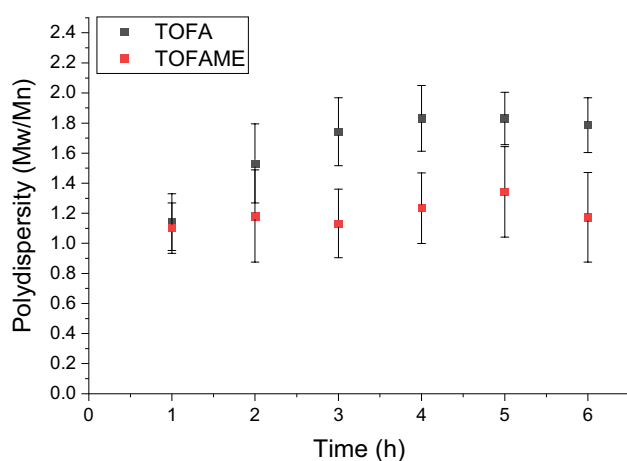The selectivity of the TOFAME epoxidation reaction was about 0.98–1.00, while the TOFA epoxidation selectivity was 0.61–0.67. It was lower due to the occurance of side reactions involving oxirane ring-opening with a carboxyl group of fatty acid. It was found that the catalyst content of 20 wt.% of is sufficient to obtain products with high EV. Increasing the catalyst content to 25 wt.% did not lead to a significant increase in EV for both TOFA and TOFAME epoxidations. A lower catalyst content can reduce the cost of the epoxidation process and is consistent with cleaner production principles. The reusability and easy separation of the catalyst from the reaction products is especially important for the cost-effectiveness of the industrial scale process [21]. The further investigation consisted of conducting ten epoxidation reactions and determining the feasibility of using ion exchange resin as a catalyst multiple times.

Figure 10 summarises the RCO and REU of 10 successive TOFA epoxidation reactions at 20 wt.% catalyst content. The results indicated good catalyst stability: the RCO was 48.2–41.9%, and the REU % was 32.2–36.3%. In a comparable experiment conducted in a batch reactor at 20 wt.% catalyst content, the RCO value after 10th reuse of the catalyst was reduced from 41.5 to 35.3% [19]. In the study by Aguilera et al. [23], the RCO of tall oil epoxidation in an isothermal batch reactor in four consecutive reactions was 42–45%.

By performing a linear approximation of the RCO and assuming a minimum value of 30% (EV approx. 0.18 mol/100 g), it can be concluded that the reusability of the catalyst in the TOFA epoxidation reaction is about 25 reactions. The use of TOFAME for the preparation of epoxidized derivatives with similar EVs to TOFA can lead to a significant extension of the catalyst lifetime.

Conclusions

A series of TOFA and TOFAME epoxidation reactions were carried out in the RBR reactor using Amberlite® IRC120 H catalyst. Results showed that methylation of TOFA allows obtaining a product with a higher
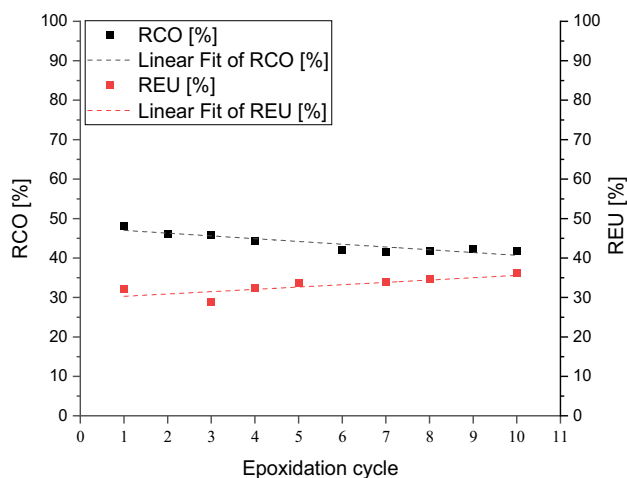

Fig. 9 Change of dispersity during epoxidation over time at the catalyst content of 25 wt.%

Table 2 Summary of the physico-chemical properties of epoxidized TOFA and TOFAME at optimal synthesis time

Catalyst content(wt.%)	Optimal synthesis time (h)	RCO (%)	REU (%)	EV (mol/100 g)	S	Viscosity (mPa•s)
TOFA epoxidation						
10	6	42.51	34.81	0.24	0.65	445.13
15	6	47.46	22.33	0.26	0.61	1442.7
20	5	49.75	27.41	0.27	0.68	723.06
25	4	51.52	24.18	0.28	0.67	472.36
TOFAME epoxidation						
10	8	65.22	33.53	0.33	0.98	36.94
15	7	78.61	23.18	0.40	~1.00	35.12
20	7	81.21	20.13	0.42	~1.00	41.26
25	7	82.34	25.15	0.42	~1.00	43.43

Fig. 10 The RCO and REU of TOFA at catalyst content of 20 wt.% of the successive cycles of epoxidation

epoxy value (TOFA: 0.223–0.281 mol/100 g; TOFAME 0.337–0.420 g/mol and smaller viscosity (TOFA: 956.93–2168.00 mPa•s; TOFAME: 36.94–54.55 mPa•s). The selectivity of TOFAME epoxidation reaction was higher than the selectivity of TOFA epoxidation. It was found that 20 wt.% of the Amberlite® IRC120 H is sufficient to obtain products with high epoxy value. Increasing the catalyst content to 25 wt.% did not significantly increase epoxy value for both TOFA and TOFAME epoxidations. Conducting the epoxidation reaction in the RBR reactor facilitated the separation process and provided the opportunity of reusing the catalyst. The Amberlite® IRC120 H catalyst was found to exhibit good stability in the TOFA epoxidation reaction. The relative conversion to oxirane decreased from 48.2 to 41.9% over 10 subsequent reactions. It was found that the conversion of double bonds to oxiranes in the TOFA epoxidation reaction carried out in the RBR reactor was higher than when a batch reactor was used. The produced TOFAME epoxy derivatives characterized by very low viscosity and high epoxy value are more suitable to be used as raw material for the synthesis of bio-polyols than TOFA epoxy derivatives.

Declarations

References

1. Satish JG, Nagesha N (2018) Cleaner production: a brief literature review. Mater Today Proc 5:17944–17951. https://doi.org/10.1016/j.matpr.2018.06.124

2. Aryan V, Kraft A (2021) The crude tall oil value chain: global availability and the influence of regional energy policies. J Clean Prod 280:124616. https://doi.org/10.1016/j.jclepro.2020.124616

3. Vevere L, Fridrihsone A, Kirpluks M, Cabulis U (2020) A review of wood biomass-based fatty acids and rosin acids use in polymeric materials. Polymers (Basel) 12:1–17. https://doi.org/10.3390/polym12112706

4. Konwar LJ, Mikkola JP, Bordoloi N et al (2018) Sidestreams from bioenergy and biorefinery complexes as a resource for circular bioeconomy. Elsevier B.V. https://doi.org/10.1016/B978-0-444-63992-9.00003-3

5. Keskin A, Yaşar A, Gürü M, Altiparmak D (2010) Usage of methyl ester of tall oil fatty acids and resinic acids as alternative diesel fuel. Energy Convers Manag 51:2863–2868. https://doi.org/10.1016/j.enconman.2010.06.025

6. Konwar LJ, Oliani B, Samikannu A et al (2022) Efficient hydrothermal deoxygenation of tall oil fatty acids into n-paraffinic hydrocarbons and alcohols in the presence of aqueous formic acid. Biomass Convers Biorefinery 12:51–62. https://doi.org/10.1007/s13399-020-01103-3

7. Knuuttila P, Kukkonen P, Hotanen U (2015) Method and apparatus for preparing fuel components from crude tall oil. US Patent No. 9024095 B2

8. Kairytė A, Kirpluks M, Ivdre A et al (2018) Cleaner production of polyurethane foam: replacement of conventional raw materials, assessment of fire resistance and environmental impact. J Clean Prod 183:760–771. https://doi.org/10.1016/j.jclepro.2018.02.164

9. Kirpluks M, Vanags E, Abolins A et al (2019) Chemo-enzymatic oxidation of tall oil fatty acids as a precursor for further polyol production. J Clean Prod 215:390–398. https://doi.org/10.1016/j.jclepro.2018.12.323

10. Sardon H, Mecerreyes D, Basterretxea A et al (2021) From lab to market: current strategies for the production of biobased polyols. ACS Sustain Chem Eng 9:10664–10677. https://doi.org/10.1021/acssuschemeng.1c02361

11. Maisonneuve L, Chollet G, Grau E, Cramail H (2016) Vegetable oils: a source of polyols for polyurethane materials.

OCL—Oilseeds fats, Crop Lipids. https://doi.org/10.1051/ocl/2016031

12. Xia Y, Larock RC (2010) Vegetable oil-based polymeric materials : synthesis, properties, and applications. Green Chem. https://doi.org/10.1039/c0gc00264j

13. Uschanov P, Heiskanen N, Mononen P et al (2008) Synthesis and characterization of tall oil fatty acids-based alkyd resins and alkyd-acrylate copolymers. Prog Org Coatings 63:92–99. https://doi.org/10.1016/j.porgcoat.2008.04.011

14. Abolins A, Pomilovskis R, Vanags E et al (2021) Impact of different epoxidation approaches of tall oil fatty acids on rigid polyurethane foam thermal insulation. Materials (Basel) 14:1–17. https://doi.org/10.3390/ma14040894

15. Meng Y, Taddeo F, Aguilera AF et al (2021) The lord of the chemical rings: catalytic synthesis of important industrial epoxide compounds. Catalysts. https://doi.org/10.3390/catal11070765

16. Omonov TS, Kharraz E, Curtis JM (2016) The epoxidation of canola oil and its derivatives. RSC Adv 6:92874–92886. https://doi.org/10.1039/c6ra17732h

17. Kirpluks M, Vanags E, Abolins A et al (2020) High functionality bio-polyols from tall oil and rigid polyurethane foams formulated solely using bio-polyols. Materials (Basel) 13:38–53. https://doi.org/10.3390/MA13081985

18. Kurańska M, Beneš H, Prociak A et al (2019) Investigation of epoxidation of used cooking oils with homogeneous and heterogeneous catalysts. J Clean Prod 236:117615. https://doi.org/10.1016/j.jclepro.2019.117615

19. Abolins A, Kirpluks M, Vanags E et al (2020) Tall oil fatty acid epoxidation using homogenous and heterogeneous phase catalysts. J Polym Environ 28:1822–1831. https://doi.org/10.1007/s10924-020-01724-9

20. Mungroo R, Pradhan NC, Goud VV, Dalai AK (2008) Epoxidation of canola oil with hydrogen peroxide catalyzed by acidic ion exchange resin. J Am Oil Chem Soc 85:887–896. https://doi.org/10.1007/s11746-008-1277-z

21. Miceli M, Frontera P, Macario A, Malara A (2021) Recovery/reuse of heterogeneous supported spent catalysts. Catalysts. https://doi.org/10.3390/catal11050591

22. Wai PT, Jiang P, Shen Y et al (2019) Catalytic developments in the epoxidation of vegetable oils and the analysis methods of epoxidized products. RSC Adv 9:38119–38136. https://doi.org/10.1039/c9ra05943a

23. Freites Aguilera A, Rahkila J, Hemming J et al (2020) Epoxidation of tall oil catalyzed by an ion exchange resin under conventional heating and microwave irradiation. Ind Eng Chem Res 59:10397–10406. https://doi.org/10.1021/acs.iecr.0c01288

24. Freites Aguilera A, Hämäläinen R, Eränen K et al (2021) Prilezhaev epoxidation of oleic acid in the presence and absence of ultrasound irradiation. J Chem Technol Biotechnol 96:1874–1881. https://doi.org/10.1002/jctb.6706

25. Lawer-Yolar G, Dawson-Andoh B, Atta-Obeng E (2021) Synthesis of biodiesel from tall oil fatty acids by homogeneous and heterogeneous catalysis. Sustain Chem 2:206–221. https://doi.org/10.3390/suschem2010012

26. Dinda S, Goud VV, Patwardhan AV, Pradhan NC (2011) Selective epoxidation of natural triglycerides using acidic ion exchange resin as catalyst. Asia-Pacific J Chem Eng 6:870–878. https://doi.org/10.1002/apj.466

27. Petrović ZS, Zlatanić A, Lava CC, Sinadinović-Fišer S (2002) Epoxidation of soybean oil in toluene with peroxoacetic and peroxoformic acids - Kinetics and side reactions. Eur J Lipid Sci Technol 104:293–299. https://doi.org/10.1002/1438-9312(200205)104:5%3c293::AID-EJLT293%3e3.0.CO;2-W

28. Musante RL, Grau RJ, Baltanás MA (2000) Kinetic of liquid-phase reactions catalyzed by acidic resins: the formation of peracetic acid for vegetable oil epoxidation. Appl Catal A Gen 197:165–173. https://doi.org/10.1016/S0926-860X(99)00547-5

29. Kousaalya AB, Beyene SD, Ayalew B, Pilla S (2019) Epoxidation kinetics of high-linolenic triglyceride catalyzed by solid acidic-ion exchange resin. Sci Rep 9:1–12. https://doi.org/10.1038/s41598-019-45458-8

30. La Scala J, Wool RP (2002) Effect of FA composition on epoxidation kinetics of TAG. JAOCS, J Am Oil Chem Soc 79:373–378. https://doi.org/10.1007/s11746-002-0491-9